



# Application of Fluid–Structure Interaction Methods to Estimate the Mechanics of Rupture in Asian Abdominal Aortic Aneurysms

Tejas Canchi<sup>1</sup> · Ashish Saxena<sup>1</sup> · EYK Ng<sup>1</sup> · Esley CH Pwee<sup>1</sup> · Sriram Narayanan<sup>2</sup>

Published online: 15 August 2018  
© Springer Science+Business Media, LLC, part of Springer Nature 2018

## Abstract

Abdominal aortic aneurysms (AAAs) occur because of dilation of the infra-renal aorta to more than 150% of its initial diameter. Progression to rupture is aided by several pathophysiological and biomechanical factors. Surgical intervention is recommended when the aneurysm maximum transverse diameter (DAAA) exceeds 55 mm. A system model that incorporates biomechanical parameters will improve prognosis and establish a relationship between AAA geometry and rupture risk. Two Asian patient-specific AAA geometries were obtained from an IRB-approved vascular database. A biomechanical model based on the fluid–structure interaction (FSI) method was developed for a small aneurysm with DAAA of 35 mm and a large aneurysm with a corresponding diameter of 75 mm. The small aneurysm (patient 1) developed a maximum principal stress (PS1) of 3.16e5 Pa and the large aneurysm (patient 2) developed a PS1 of 2.32e5 Pa. Maximum deformation of arterial wall was 0.0020 m and 0.0022 m for patients 1 and 2 respectively. Location of maximum integral wall shear stress (WSS) (fluid) was different from that of PS1. Induced WSS was also higher in patient 1 (18.74 Pa vs 12.88 Pa). An FSI model incorporating the effect of both the structural and fluid domains aids in better understanding of the mechanics of AAA rupture. Patient 1, having a lower DAAA than patient 2, developed a larger PS1 and WSS. It may be concluded that DAAA may not be the sole determinant of AAA rupture risk.

**Keywords** Abdominal aortic aneurysm · Fluid–structure interaction · Asian patient geometry · Rupture risk · Patient-specific

## 1 Introduction

Abdominal aortic aneurysm (AAA) is a vascular condition that affects the elderly population, mainly above the age of 55. It is a highly asymptomatic disease where the infra-renal aorta progressively dilates to more than two times its original diameter. Non-intervention leads to weakening of the arterial wall and rupture (Fig. 1). In the event of a rupture, mortality is high. Pathophysiological and biomechanical factors contribute to the genesis, growth, and rupture of the AAA. These include advanced age, greater height, coronary artery disease, atherosclerosis, high cholesterol levels, hypertension [1], and smoking [2, 3]. The clinical metric used for surgical intervention is the

maximum transverse diameter (DAAA). The DAAA, being the diameter of the AAA lumen, was measured along the central lateral axis. Clinicians have used a value of 55 mm as the threshold for DAAA to recommend surgical intervention. But this metric has been seen to be inadequate in many cases [4]. Hence, a biomechanics-based approach is essential to accurately assess the risk of rupture of AAA.

Biomechanical parameters such as principal stresses and wall shear stresses are significant in the progression to rupture of the arterial wall. This was first proposed by Vorp et al. in 1998 [5] in which they argued that the use of wall stress in the lumen can predict the rupture of AAA more accurately than just the DAAA. Additional factors drawn from the morphology of the AAA are also correlated to these biomechanical factors. This has been established by Chauhan et al. in 2017 [6] where they demonstrated that certain geometric parameters of the ruptured AAA are highly correlated to the peak wall stress which is an indicator of AAA rupture. They demonstrated that the set of geometric indices can predict the stresses to a higher percentage than by just using the maximum diameter as a metric to assess rupture risk.

There have been numerous studies quantifying the incidence of AAA in the Caucasian population; retrospective studies have looked at the Asian demographic in several

✉ EYK Ng  
mykng@ntu.edu.sg

<sup>1</sup> School of Mechanical and Aerospace Engineering, Nanyang Technological University, 50 Nanyang Avenue, Singapore 639798, Singapore

<sup>2</sup> Department of General Surgery, Tan Tock Seng Hospital, Singapore, Singapore

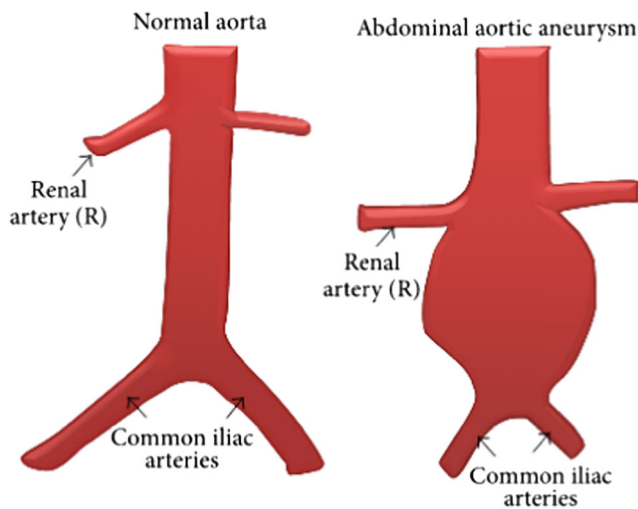


**Fig. 1** Normal abdominal aorta and abdominal aortic aneurysm

locations to bring out the incidence of AAA in the Asian population. Li et al. [7] reported prevalence of AAA considering 56 studies. The prevalence in Asians was 0.5% as against 2.2% for American patients and 2.5% for European patients. This has been corroborated by Guo and Zhang [8], where in a study covering 23,810 patients, the prevalence was seen to be 0.11%. The incidence in Chinese men was 0.18% whereas it was 0.07% in Chinese women. Other studies done earlier in Japan reported incidence of about 0.36% [9, 10], while in Korea, it has been seen to be 0.55% [11]. In a study done in Malaysia, Yii [12] reported that among 123 patients in the Sarawak region of Borneo, incidence among high-risk males and females was 25.6 and 7.6 per 100,000. In the Caucasian population, a similar metric has shown a range from 3.0 to 117.2 per 100,000.

Additionally, it has been determined through clinical and statistical analysis that the morphology of the Asian aorta is distinct when compared to its Caucasian counterpart. It has been reported that the stent grafts used for the endovascular aneurysm repair (EVAR) process are unsuitable for Asian populations as against the Caucasian ones. A stent graft is difficult to place if the proximal neck of the aneurysm is shorter than 1.5 cm. In addition, the angle between the neck of the aneurysm and the sagittal plane of the aorta must not be less than 60° or cone-shaped, the iliac arteries must not be tortuous, and their diameter must be at least 8 mm. All available commercial stents are designed for the Caucasian aortal dimensions, and hence, clinicians in Asia have a problem in adjusting them for the Asian aorta.

In a clinical investigation to compare three commercially available stents, Cheng et al. [13] carried out a spiral CT and angiographic assessment of 65 Chinese (58 men, mean age 74 years, range 50–87) who underwent EVAR. The morphological parameters were compared with European and American patients. It was found that the common iliac arteries (CIAs) were significantly shorter in Asians, particularly on the right-hand side. The right CIA had a mean length of 29.9 mm

while the left had a mean length of 34.2 mm compared to more than 50 mm in the Caucasian samples. The distance between the lowest renal artery and the CIA bifurcation averaged 20 mm shorter in Asians: 148 mm on the right side and 153 mm for the left. The CIAs were also wider, averaging 20.2 mm for the right and 17.9 mm for the left. This was reinforced in an investigation carried out by Mladenovic et al. [14] who investigated the difference in Asian and European patients' histories along with their aneurismal morphological features to aid in the clinical use of endovascular stent grafts. They concluded that the European patient group had longer CIAs as before with 47.41 mm in Asians and 59.68 in Europeans. The AAA mean neck length in Asians was seen at 22.73 mm and 38.72 mm in Europeans. The mean AAA length was not statistically significant though with 104.97 mm in Asians against 108.24 mm in Europeans. These differences in morphology can cause changes in the flow physics in the diseased lumen. A biomechanical analysis of the Asian aorta would be therefore useful in understanding the changes in progression of the disease in the patients and aid the design of a stent graft that might be specifically designed for Asian morphology.

Computational methods-based analyses have been carried out using solid mechanics, fluid mechanics, or a combination of these, known as fluid–structure interaction. Computational solid mechanics-based equations have been used to quantify stress development in the arterial wall [15–18]. Initial forays considered only the fluid or the solid mechanics of the AAA separately through CFD and FEA methods as listed before. But the arterial wall is not rigid as it responds to the blood flow in the artery. This fluid–structure interaction (FSI) is bi-directional. Accounting for FSI provides a suitable approach to the most physiologically accurate solution. This was first investigated by DiMartino et al. [19] using an Arbitrary Lagrangian–Eulerian (ALE) method to accurately determine a FSI solution. Additional studies carried out by Scotti et al. in 2005 and 2008 [20, 21] that considered the movement of the wall overestimated the stress values by 20% as against a rigid simulation and applying a varying wall thickness also increased the von Mises stress in the aneurysm model. This was reinforced by Papaharilaou et al. [22] who reported a 12.5% difference in peak stress when a decoupled FSI solution was incorporated. Figueroa [23] formulated a coupled momentum method (CMM) for FSI problems using stabilized FEM. He investigated flow in the AAA under rest and exercise conditions to quantify changes in stress, observing that during exercise, the deformation of the wall is no longer occurring in a radial expansion and contraction fashion, but rather as a net motion forward and backwards due to the much larger inertial forces exerted on the wall by the impinging blood stream. Li and Kleinstreuer [24] in an FSI study observed that a large neck angle of the aneurysm may cause strong irregular vortices in the AAA cavity and may influence the wall stress distribution by increasing it as much as 40%. The rupture

risk of lateral asymmetric AAAs is higher than for the anterior–posterior asymmetric types. The most likely rupture site is located near the anterior distal side for the anterior–posterior asymmetric AAA and the left distal side in the lateral asymmetric AAA. The incorporation of asymmetry is important as Fraser et al. [25] reported differences in stress between a rigid walled calculation and FSI to be less than 3.5%. But this analysis was carried out using an axisymmetric AAA model.

As has been seen from prior studies, FSI analysis provides a more realistic picture of the stresses induced in AAA. It provides insight into the mechanics of rupture by considering both the structural and fluid solutions as against exclusively one of them, or even the use of only maximum transverse diameter as a metric to determine rupture.

This work set out to investigate the efficacy of using the maximum transverse diameter metric in the determination of AAA rupture risk in Asian patients. To this end, patient AAAs that have a maximum transverse diameter of 3.5 cm and 7.5 cm that were on either side of the clinical metric of 5.5 cm were used in the analysis. The morphology of the Asian aorta being different from that of the Caucasian aorta merits further investigation of the mechanics of rupture and this work is an initial study towards that aim. The novelty is brought out in terms of demonstrating the incorporation of FSI as a method to determine the rupture risk accurately in the Asian AAA.

In this paper, two Asian patient AAAs are subjected to FSI analysis to determine a measure of the rupture risk. This will be done by extracting the principal stresses induced in the arterial wall and the corresponding wall shear stresses by the blood flow. A comparison of these two patient AAAs will also be made to deduce any relationship between the AAA geometry and the stresses developed.

## 2 Methods

### 2.1 Geometry

Two patient-specific AAA computed tomography angiographies originated from Singapore were obtained from Tan Tock Seng Hospital, Singapore's IRB-approved vascular database. The imaging protocol followed was the clinical standard for vascular intervention. The CT images were obtained at a slice distance of 1 mm with a single breath hold using a 128-slice Phillips CT scanner. One was a large aneurysm with a DAAA of 75 mm, while the other, a small aneurysm having a DAAA of 35 mm. The obtained patient CTs were subjected to level set segmentation using the open-source application ITKSnap [26]. The resulting geometry was then smoothed using MeshLab [27], an open-source application where a series of Poisson filters were used to rid it of artifacts. The resulting *stl* file was exported to SolidWorks (Dassault Systemes

Corporation, Waltham, MA) wherein a constant thickness of 2 mm was added to make it suitable for meshing for an FSI problem. Meshing was carried out using the commercial software ICEMCFD in ANSYS Workbench 16.1 (Canonsburg, PA). The intra-luminal thrombus (ILT) was not considered in this geometric model. Tetrahedral mesh was created for the structural wall and the fluid mesh would be a volumetric hexahedral mesh in both cases. The meshes are shown in Figs. 2a and 2b.

### 2.2 Governing Equations

The properties of blood in the simulations were assumed to be Newtonian and incompressible. The Newtonian assumption for blood has been seen to be consistent for large arteries [28]. The inlet flow was made pulsatile to be physiologically accurate. Fluid–structure coupling of the aneurysmal wall motion and blood flow is made using the Arbitrary–Lagrangian Eulerian (ALE) method. The incompressible continuity and the Navier–Stokes equations in ALE form can be expressed as

$$\nabla \times u = 0$$

$$\rho_f \left( \frac{\partial u}{\partial t} + ((u - u_g) \times \cdot \nabla) u \right) = -\nabla p + \mu \nabla^2 u$$

where  $\rho_f$ ,  $p$ ,  $u$ , and  $u_g$  are the fluid density, the pressure, the fluid velocity, and the moving coordinate velocity, respectively. In ALE formulation, the term  $(u - u_g)$ , which is the relative velocity of the fluid with respect to the moving coordinate velocity, is added to the conventional Navier–Stokes equations to account for movement of the mesh [29].

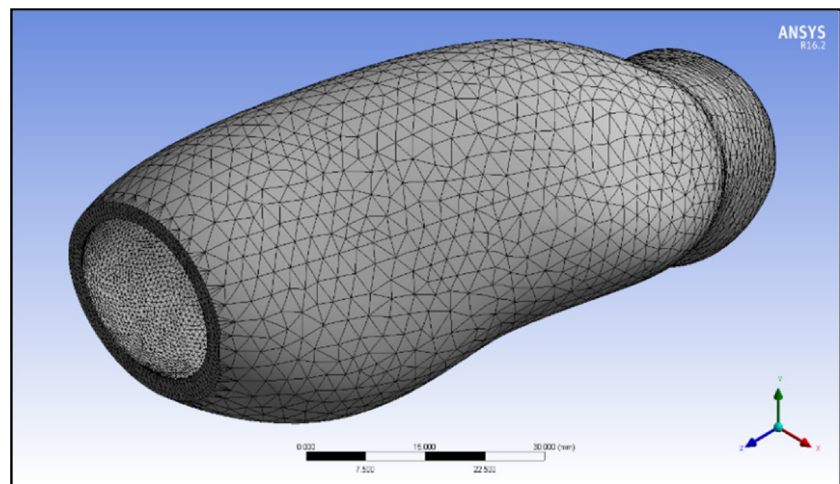
### 2.3 Numerical Procedure

The FSI method is applied to the patient AAAs using the commercial finite volume solver, ANSYS 16.1 Workbench which incorporates the ALE method in its system coupling function. The system coupling was carried out between ANSYS Mechanical on the structural side and FLUENT on the fluid side. User-defined functions (UDFs) were used to input the inlet velocity and outlet pressure boundary conditions. The values of  $\rho$  and  $\mu$  were taken to be 1060 kg/m<sup>3</sup> and 0.0035 Pa-s for blood. The SIMPLE method [30] was used with a time step calculated assuming the heart rate to be 72 beats per minute for the transient fluid solution. The simulation was carried out for three cardiac cycles, each cycle consisting of 500 time steps. The convergence criteria were set to 1e-04 for the continuity and momentum equations.

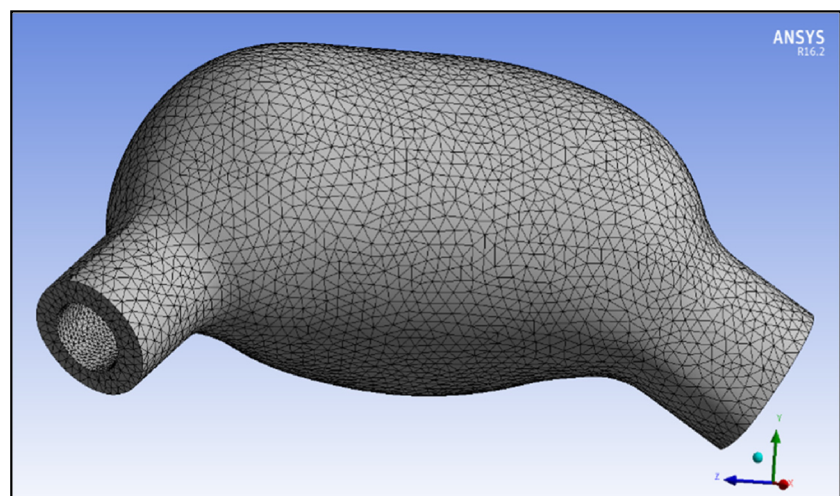
### 2.4 Boundary Conditions and Material Properties

The inlet and outlet boundary conditions were defined to be pulsatile with waveforms being extracted from literature [31].

**Fig. 2** **a** Structural mesh of AAA geometry from patient 1. **b** Structural mesh of AAA geometry from patient 2



(a)



(b)

The walls were bound by a no-slip condition and a FSI interface was defined at the inner wall of the aneurysm lumen, through the system coupling function of ANSYS Workbench. Figures 3a, 3b show the inlet velocity and outlet pressure boundary conditions. For the arterial wall, the density was taken to be  $1120 \text{ kg/m}^3$  [32]. By assuming isotropic elasticity, the value of the Young's modulus was taken to be 4.5 MPa and Poisson's ratio to be 0.45 [33]. The boundary conditions were input through a UDF script in ANSYS. The boundary conditions were kept the same for both patients so as to allow comparison of the extracted biomechanical parameters.

## 2.5 Independence Studies

As part of the verification process, three different mesh sizes were investigated for mesh independence of the solver. The integral wall shear stress in the fluid was chosen as the parameter of interest in the study for both patients. The systole occurred at 2.18 s for patient 1 and 2.3 s for patient 2. The

maximum integral wall shear stress was then recorded at systole for all mesh sizes in both the patients. As seen from Tables 1 and 2, the solutions were indeed independent of mesh size. In patient 1, the fine mesh size showed a difference of 4.16% in the integral wall shear stress while the coarse mesh saw no error. In patient 2, as compared to the initial normal mesh size, the coarse mesh size saw a variation of the integral wall shear stress of about 2.81%, whereas it was lower at 0.56% when the fine mesh was used. The least mesh size that was not computationally expensive was used in each case for the FSI simulation. For patient 1, the 2.2 million element mesh and for patient 2, the 1.69 million element mesh were used in the final simulations.

## 3 Results and Discussion

The present study is an attempt to estimate the mechanics of rupture of Asian AAA using FSI methods. Even though incidence is low in Asian patients, it is important to establish the

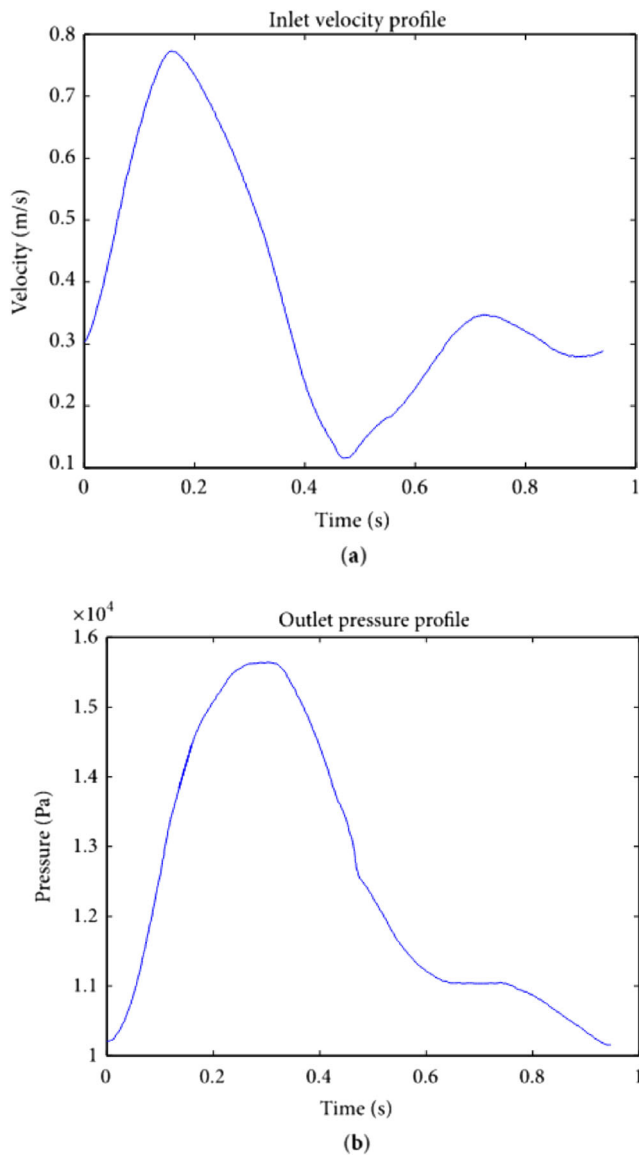


**Fig. 3** **a** Inlet velocity boundary condition waveform. **b** Outlet pressure boundary condition waveform

biomechanics of the Asian AAA cohort and eventually improve point-of-care technologies for them. FSI analysis of the Asian AAA will aid this pursuit. The arterial wall being a non-rigid entity is subject to interaction with the fluid flow and vice versa. Hence, this requires a FSI solution to investigate the effects of the

**Table 1** Independence studies (patient 1)

Mesh size	Number of elements (millions)	Maximum integral wall shear stress at systole in third cardiac cycle (Pa)	Percentage difference to normal mesh
Fine	3.34	0.024	0
Normal	2.02	0.024	0
Coarse	0.80	0.023	4.16

**Table 2** Independence studies (patient 2)

Mesh size	Number of elements (millions)	Maximum integral wall shear stress at systole in third cardiac cycle (Pa)	Percentage difference to normal mesh
Fine	4.96	0.0365	2.81
Normal	3.14	0.0355	0
Coarse	1.69	0.0353	0.56

moving arterial wall in the estimation of rupture risk as it incorporates the material properties of the arterial wall.

The deformation, maximum principal stress, and maximum shear stresses were extracted in the structural domain while the integral wall shear stress was the parameter of interest in the fluid domain. Also, the velocity streamlines and pressure distribution over the arterial wall was quantified in each patient. FSI simulations were carried out for three cardiac cycles measuring 0.9 s each. The plots were generated at systole in the third cardiac cycle. This was done to damp out any initial transients resulting from the computational method.

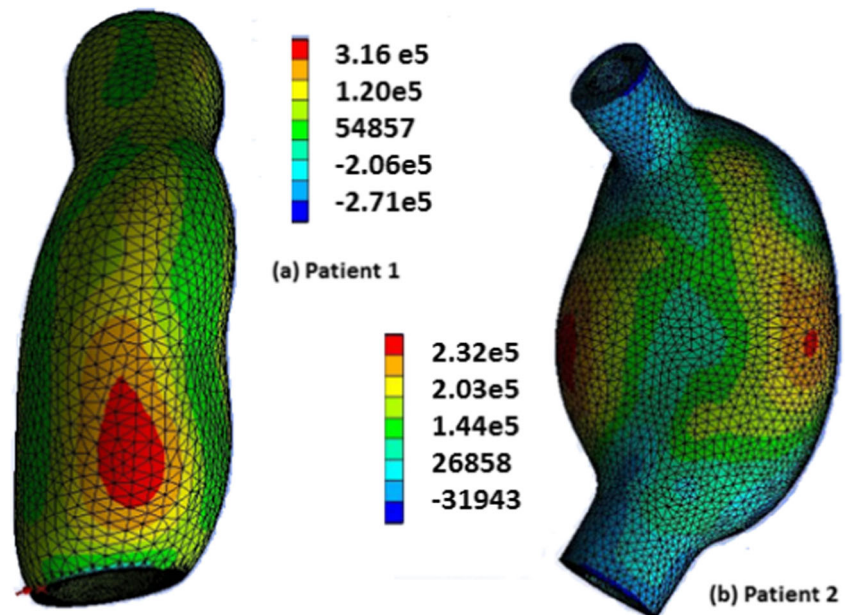
The parameters that caused the most effect on the risk of rupture of the AAA were first principal stress and wall shear stress. This was established from the maximum principal stress theory and maximum shear stress theory that are failure theories in mechanics. In the maximum principal stress theory, the material would fail if the maximum principal stress induced exceeds the maximum normal strength of the material. As for the maximum shear stress theory, the material would fail if the maximum shear stress suffered exceeds the maximum allowable shear stress.

Hence, it is important to observe the results of the maximum shear and principal stresses in the structural domain to comment on the rupture risk. In the same manner, the wall shear stress, induced in the fluid domain, would be important affecting the results in the structural domain in a strongly coupled solution.

### 3.1 First Principal Stress (Structural Domain)

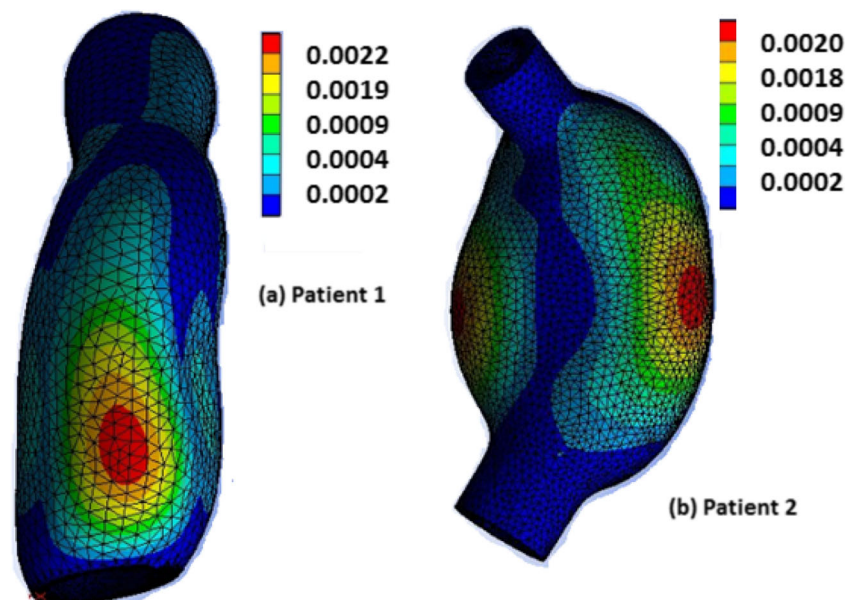
The first principal stress is a suitable metric to determine the peak stress that is being induced in the arterial wall. Principal stresses are the normal stress acting on the arterial wall. The force acting on the arterial wall is the pressure load from the fluid, and hence, the principal stresses are the indicators of the stress distribution that may lead to rupture of the wall. The location of the highest principal stresses on the arterial wall is usually seen to be in the antero-distal region of the AAA lumen. Figure 4 shows the distribution of the first principal stresses in each patient. As seen from the figure, the regions of maximum principal stress induced in each of the patients are clearly marked out as the ones in red. In patient 1, the region is seen to be more distal than that for patient 2. From structural failure

**Fig. 4** Spatial distribution of first principal stresses at the AAA wall (Pa)



theories, we can deduce that these regions may be most susceptible to rupture. The principal stresses show a marked difference in each patient as seen from Fig. 4. While the small AAA (patient 1) shows a maximum principal stress of 0.3 MPa, the larger aneurysm shows a lesser maximum principal stress at only 0.22 MPa. This brings out the importance of quantifying the biomechanical stress as opposed to only the maximum transverse diameter of the AAA as a metric for surgical intervention by clinicians. In this case, patient 1 has a higher stress and may be at a higher risk even though the maximum transverse diameter is well below the clinical threshold of 55 mm. The maximum principal stresses in Caucasian patients have been used as a metric by Scotti and others [20, 21] successfully to establish rupture potential in AAAs in their FEA analysis.

**Fig. 5** Spatial distribution of the AAA wall deformation (m)

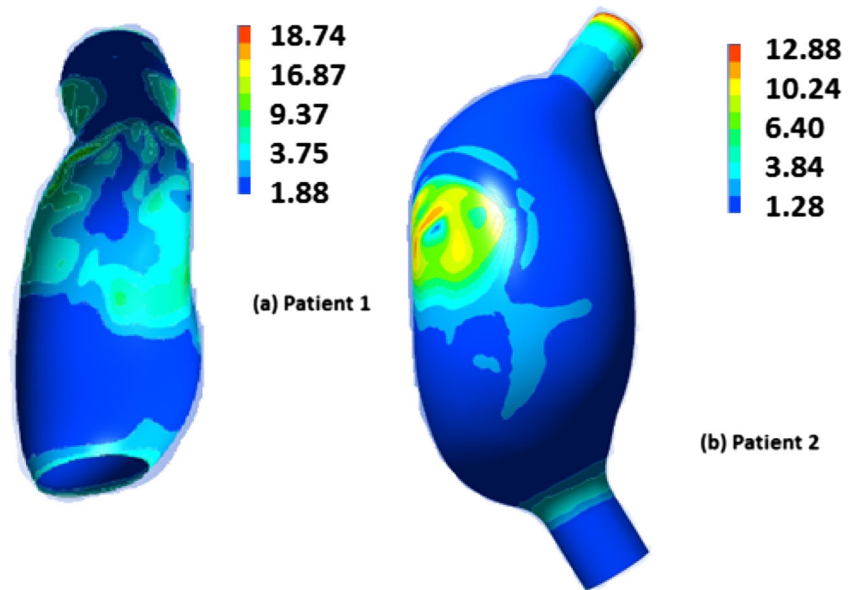


The ranges of principal stresses developed in both the patient aortas in the present analysis are in the same range as those induced in Caucasian AAAs (0.2–0.4 MPa). While this may be expected, as Chauhan et al. [6] have reported, the morphological characteristics can have an effect on the estimation of biomechanical stresses in the AAA. This merits further investigation on a larger cohort of patients where FSI and geometric quantification are done congruently to assess rupture risk.

### 3.2 Structural Deformation

This study accounts for the interaction between the fluid and the structure considering the arterial wall as a non-rigid entity. The ALE method that involves a strongly

**Fig. 6** Spatial distribution of WSS (fluid) on the arterial wall (Pa)



coupled solution exchanges the structural deformation value with the fluid in every time step. The structural deformation value is an important parameter in the simulation. The maximum deformation of the arterial wall is visualized in Fig. 5. Quantitatively, there is little difference in the maximum values of the deformation in both the patients. The maximum deformation value in patient 1 is 0.0022 m while it is 0.0020 m in patient 2. The location of maximum deformation is aligned with the location of the maximum principal stresses in both the patients. As the arterial wall is weakened during the progression of the disease, the deformation at the site of the high principal stress promotes the tendency to rupture.

### 3.3 Wall Shear Stress (Fluid Domain)

Wall shear stress is induced by the fluid on the arterial wall. The values of wall shear stress (WSS) are extracted from the fluid solution in the FSI simulation. It is a challenge to quantify the WSS in vivo, and hence, computational methods must be used. Figure 6 shows the comparison of the induced WSS in both models. The peak WSS on the arterial wall, induced in patient 1, is 18.74 Pa as against patient 2 where only 12.88 Pa is induced on the arterial wall. Also seen from the figure, the location of peak wall shear stress is not at the same location as that of the peak first principal stress. It is also clear from the pressure distribution that the sites of integral wall shear stress

**Fig. 7** Velocity streamlines in the fluid domain (m/s)

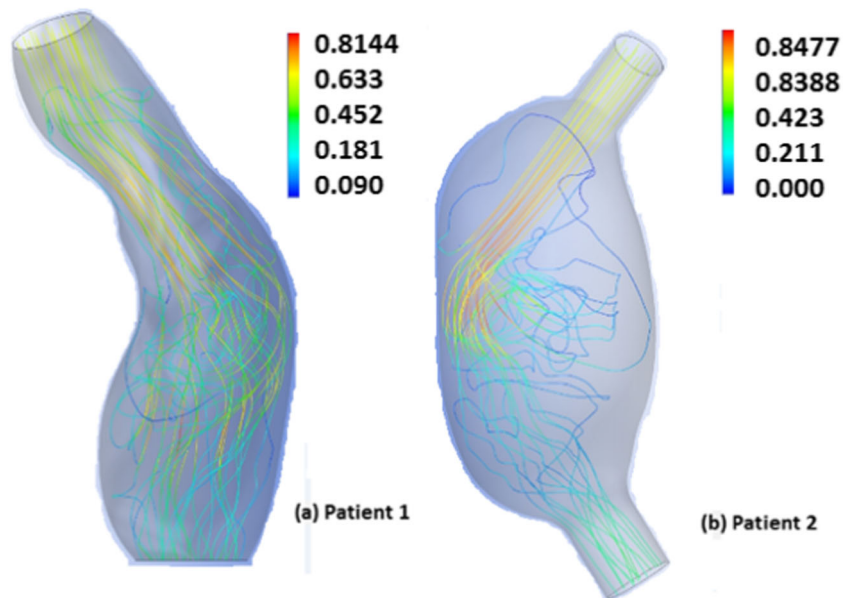
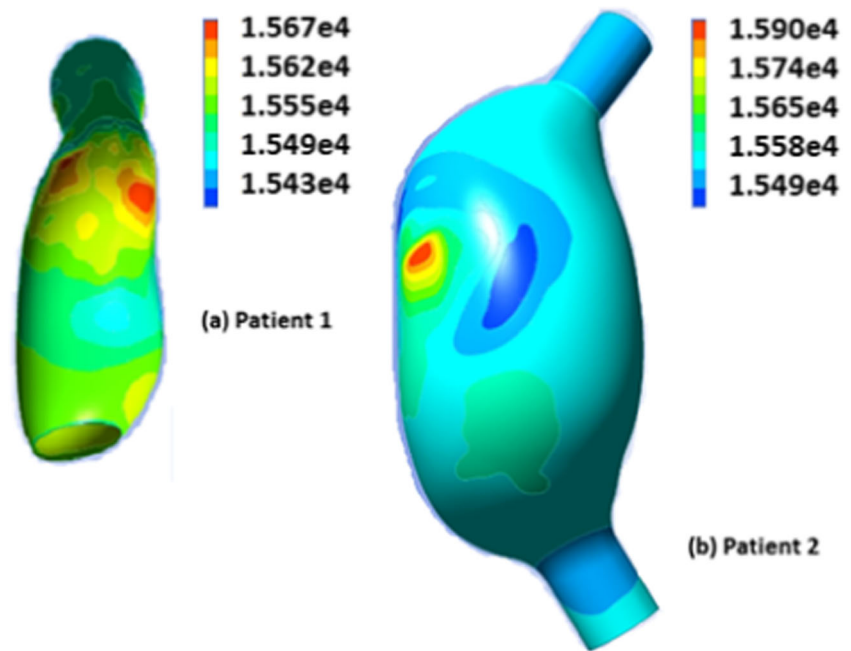


**Fig. 8** Pressure distribution in the fluid domain (Pa)



and the pressure are correlated. This is supported by Boyd et al. [34] who reported that low wall shear stresses dominate sites of rupture in AAA.

### 3.4 Velocity and Pressure (Fluid Domain)

Velocity streamlines were extracted using the post-processing application, CFD-Post, that is part of the ANSYS workbench suite. The streamlines provide insight into how the fluid is inducing pressure on the arterial wall. The changed geometry of the diseased aorta as compared to the healthy aorta induces vorticity in the fluid. Flow vortices that are formed at the beginning of the cycle due to the geometry of the aneurysm migrate distally as the flow decelerates from peak systolic conditions to diastole. Initially, there is attached flow near the proximal end of the aneurysm but by peak systole there is a separation of the vortices from the wall. This is seen in the streamlines generated for both the patients. The flow separation is higher in the larger aneurysm of patient 2 as there is a pronounced neck region that induces the flow to turn the corner (Fig. 7). This effect is lesser in the smaller aneurysm as there is a relatively less visible neck region and the lumen curvature is lower as the fluid moves from the proximal to the distal region of the AAA model.

Figure 8 shows the distribution of pressure over the arterial wall as computed in the fluid domain. When compared to the

structural stress distribution, it is seen that the sites of the highest structural stresses were not found to be the same as those having irregular vortical flow or those with high fluid WSS. One possible reason could be that as the arterial wall is treated as a non-rigid entity, it has non-uniform stress distributions due to the pulsatile nature of flow in the lumen.

## 4 Patient Model Comparison

In this study, a small aneurysm and a large aneurysm are investigated from the Asian cohort to establish the biomechanics of the Asian AAA. These two patient models are suitable cases for comparing the biomechanics of rupture as the maximum transverse diameters are on either side of the clinical metric of 55 mm. Quantification of stresses developed in these two patients would provide insight into the mechanics of rupture where clinicians have been recommending surveillance or immediate surgery, as in the case of a small or a large aneurysm, respectively.

Table 3 compares the two patient models in terms of the stresses developed in both the fluid and structural domains. From the table, it can be observed that patient 1 had a larger value of maximum shear stress and maximum principal stress. These parameters were the determining factors that affect failure of the AAA in the structural domain. The site of the

**Table 3** Comparison of biomechanical parameters from patients 1 and 2

Parameters/patient	Maximum shear stress (Pa)	Maximum principal stress (Pa)	Total deformation (m)
Patient 1	1.65e5	3.16e5	0.0020
Patient 2	1.21e5	2.32e5	0.0022



highest stresses would then be the most probable location where rupture would occur. However, rupture would only occur if the stresses indicated in Figs. 4 and 6 are higher than the aorta wall maximum normal strength and maximum allowable shear stress respectively.

It can be deduced from the results obtained from the FSI analysis that patient 2 with a much larger AAA size would have a lower chance of rupture risk as compared to patient 1 under these simulation conditions. This implies that the size of AAA may not be the sole determinant of the risk of rupture.

## 5 Conclusions

This study is the first of its kind to aim at establishing the biomechanical parameters for Asian AAA using a FSI-based computational model. As has been established from literature, the incidence of AAA in Asians is low. But as there is prevalence, it is important to establish a biomechanical model for the Asian AAA. This has been done here using an FSI method that incorporated the movement of the arterial wall and its interaction with the blood flow in the AAA lumen in two patient-specific Asian patient geometries.

A two-way FSI problem was formulated based on boundary conditions extracted from literature for each of the two patient models. To carry out a comparison of the mechanics of rupture in each of the two patients, biomechanical stress parameters such as maximum first principal stress and total deformation in the structural domain and integral wall shear stress along with pressure and velocity correlations were analyzed in the fluid domain. A comparison of stresses induced showed that the values of principal stresses (structural domain) in the smaller aneurysm model were higher than those for the bigger aneurysm (3.16e5 vs 2.32e5 Pa). This was also true in the fluid domain (18.74 vs 12.88 Pa). Additionally, the biomechanical stresses developed by the AAA models are in the same range of values as those of Caucasian AAAs. It has been established that the morphological characteristics of the Asian AAA are different from those of the Caucasian AAA. Hence, a study that incorporates the morphological differences through quantification of geometric indices is warranted.

From this study, it may be concluded that the maximum transverse diameter alone may not be the sole determinant of rupture risk. Incorporating the biomechanics in the prognosis could be a step forward in minimizing the risk of surgical intervention and bring down healthcare costs. This is an initial study into the mechanics of rupture in Asian AAA and there will be subsequent studies on a larger patient cohort.

**Acknowledgements** Tejas Canchi acknowledges receipt of the Research Student Scholarship from the Lee Kong Chian School of Medicine, Nanyang Technological University, Singapore.

## Compliance with Ethical Standards

**Conflict of Interest** The authors declare that they have no conflict of interest.

## References

- Kent, C. K., Zwolak, R. M., Egorova, N. N., et al. (2010). Analysis of risk factors for abdominal aortic aneurysm in a cohort of more than 3 million individuals. *Journal of Vascular Surgery*, 52(3), 539–549.
- Lederle, F. A., Johnson, G. R., Wilson, S. E., et al. (2000). The aneurysm detection and management study screening program: validation cohort and final results. Aneurysm Detection and Management Veterans Affairs Cooperative Study Investigators. *Archives of Internal Medicine*, 160(10), 1425–1430.
- Chaikof, E. L. (2009). The care of patients with an abdominal aortic aneurysm: the Society for Vascular Surgery practice guidelines. *Journal of Vascular Surgery*, 50(8S), 2S–49S.
- Van de Geest, J. P., et al. (2006). A biomechanics-based rupture potential index for abdominal aortic aneurysm risk assessment. *Annals of the New York Academy of Sciences*, 1085(1), 11–21.
- Vorp, D. A., Raghavan, M. L., & Webster, M. W. (1998). Mechanical wall stress in abdominal aortic aneurysm: influence of diameter and asymmetry. *Journal of Vascular Surgery*, 27(4), 632–639.
- Chauhan, S. S., et al. (2017). The association between geometry and wall stress in emergently repaired abdominal aortic aneurysms. *Annals of Biomedical Engineering*, 45(8), 1908–1916.
- Li, X., Zhao, G., Zhang, J., Duan, Z., & Xin, S. (2013). Prevalence and trends of the abdominal aortic aneurysms epidemic in general population – a meta-analysis. *PLoS ONE*, 8(12), e81260. <https://doi.org/10.1371/journal.pone.0081260>.
- Guo, W., & Zhang, T. (2014). Abdominal aortic aneurysm prevalence in China. *Endovascular Today*, 76–82.
- Adachi, K., Iwasawa, T., & Ono, T. (2000). Screening for abdominal aortic aneurysms during a basic medical checkup in residents of a Japanese rural community. *Surgery Today*, 30, 594–599.
- Ishikawa, S., Ohtaki, A., Takahashi, T., et al. (2001). The characteristics of screened patients with abdominal aortic aneurysms. *International Angiology*, 20, 74–77.
- Oh, S. H., Chang, S. A., Jang, S. Y., et al. (2010). Routine screening for abdominal aortic aneurysm during clinical transthoracic echocardiography in a Korean population. *Echocard*, 27, 1182–1187.
- Yii, M. K. (2003). Epidemiology of abdominal aortic aneurysm in an Asian population. *ANZ Journal of Surgery*, 73, 393–395.
- Cheng, S. W. K., et al. (2004). Aortic aneurysm morphology in Asians: features affecting stent-graft application and design. *Journal of Endovascular Therapy*, 11(6), 605–612.
- Mladenovic, A. S., Markovic, Z. Z., & Hyodoh, H. H. (2012). Anatomic differences of the distal aorta with dilatation or aneurysm between patients from Asia and Europe as seen on CT imaging. *European Journal of Radiology*, 81(9), 1990–1997.
- Rodríguez, J. F., et al. (2008). Mechanical stresses in abdominal aortic aneurysms: influence of diameter, asymmetry, and material anisotropy. *Journal of Biomechanical Engineering*, 130(2), 021023.
- Rodríguez, J. F., et al. (2009). The effect of material model formulation in the stress analysis of abdominal aortic aneurysms. *Annals of Biomedical Engineering*, 37(11), 2218–2221.
- Tong, J., et al. (2011). Effects of age on the elastic properties of the intraluminal thrombus and the thrombus-covered wall in abdominal aortic aneurysms: biaxial extension behaviour and material

- modelling. *European Journal of Vascular and Endovascular Surgery*, 42(2), 207–219.
18. Gasser, T. C. (2011). An irreversible constitutive model for fibrous soft biological tissue: a 3-D microfiber approach with demonstrative application to abdominal aortic aneurysms. *Acta Biomaterialia*, 7(6), 2457–2466.
  19. DiMartino, E. S., et al. (2001). Fluid–structure interaction within realistic three-dimensional models of the aneurysmatic aorta as a guidance to assess the risk of rupture of the aneurysm. *Medical Engineering & Physics*, 23(9), 647–655.
  20. Scotti, C. M., et al. (2005). Fluid-structure interaction in abdominal aortic aneurysms: effects of asymmetry and wall thickness. *Biomedical Engineering Online*, 4(1).
  21. Scotti, C. M., et al. (2008). Wall stress and flow dynamics in abdominal aortic aneurysms: finite element analysis vs. fluid–structure interaction. *Computer Methods in Biomechanics and Biomedical Engineering*, 11(3), 301–322.
  22. Papaharilaou, Y., et al. (2007). A decoupled fluid structure approach for estimating wall stress in abdominal aortic aneurysms. *Journal of Biomechanics*, 40, 367–377.
  23. Figueroa, C. A. (2006) A coupled-momentum method to model blood flow and vessel deformation in human arteries: applications in disease research and simulation-based medical planning. Doctoral dissertation, Stanford University.
  24. Li, Z. H., & Kleinstreuer, C. (2007). A comparison between different asymmetric abdominal aortic aneurysm morphologies employing computational fluid-structure interaction analysis. *European Journal of Mechanics - B: Fluids*, 26(5), 615–631.
  25. Fraser, K. H., Li, M. X., Lee, W. T., Easson, W. J., & Hoskins, P. R. (2009). Fluid-structure interaction in axially symmetric models of abdominal aortic aneurysms. Proceedings of the Institution of Mechanical Engineers. Part H. *Journal of Engineering in Medicine*, 223(2), 195–209.
  26. Yushkevich, P. A., et al. (2006). User-guided 3D active contour segmentation of anatomical structures: significantly improved efficiency and reliability. *Neuroimage*, 31(3), 1116–1128.
  27. Cignoni P, Callieri M, Corsini M et al (2008) MeshLab: an open-source mesh processing tool. Sixth Eurographics Italian Chapter Conference, 129–136.
  28. Ross, E. C., & Simmons, C. A. (2007). *Introductory biomechanics: from cells to organisms*. Cambridge University Press.
  29. Canchi, T., et al. (2015). A review of computational methods to predict the risk of rupture of abdominal aortic aneurysms. *BioMed Research International*, 2015, 861627.
  30. Patankar SV (1980) Numerical heat transfer and fluid flow. Taylor & Francis.
  31. Soudah, E., Ng, E. Y., Loong, T. H., Bordone, M., Pua, U., & Narayanan, S. (2013) CFD modelling of abdominal aortic aneurysm on hemodynamic loads using a realistic geometry with CT. *Computational and Mathematical Methods in Medicine*, 2013, 9.
  32. Pasta, S., et al. (2013). Difference in hemodynamic and wall stress of ascending thoracic aortic aneurysms with bicuspid and tricuspid aortic valve. *Journal of Biomechanics*, 46(10), 1729–1738.
  33. Giannakoulas, G., et al. (2005). A computational model to predict aortic wall stresses in patients with systolic arterial hypertension. *Medical Hypotheses*, 65(6), 1191–1195.
  34. Boyd, A. J., et al. (2016). Low wall shear stress predominates at sites of abdominal aortic aneurysm rupture. *Journal of Vascular Surgery*, 63(6), 1613–1619.